PERGAMON

International Journal of Solids and Structures 40 (2003) 2041–2056

INTERNATIONAL JOURNAL OF SOLIDS and STRUCTURES

www.elsevier.com/locate/ijsolstr

A piezoelectric screw dislocation near a wedge-shaped bi-material interface

B.J. Chen, Z.M. Xiao *, K.M. Liew

School of Mechanical and Production Engineering, Nanyang Technological University, Nanyang Avenue, Singapore 639798, Singapore

Received 4 October 2002

Abstract

The electro-elastic stress field due to a piezoelectric screw dislocation near the tip of a wedge-shaped bi-material interface is derived. The screw dislocation is subjected to a line charge and a line force at the core. The explicit closed-form analytical solutions for the stress field are derived by means of the complex variable and conformal mapping methods. The stress and electric intensity factors of the wedge tip induced by the dislocation and the image force acting on the dislocation are also formulated and calculated. The influence of the wedge angle and the different bi-material constant combinations on the image force is discussed. Numerical results for three particular wedge angles are calculated and compared.

Keywords: Dislocation; Wedge-shaped interface; Interaction; Stress and electric intensity factor; Force on dislocation

1. Introduction

In engineering materials and structures, wedge-shaped interfaces are very often encountered, such as in polycrystalline materials, composite materials with irregular inclusions, and square silicon die encapsulated by epoxy matrix in electronic packages, etc. As a wedge-shaped interface introduces a stress singularity at its corner where a micro-crack could be easily initiated, it is important to analyze such kind of problems. Bogy and Wang (1971) investigated the problem of a composite body consisting of two dissimilar isotropic, homogeneous wedges. In their work, an eigen equation for determining the order of singularity at the corner of wedge shaped interface was given. The same problem was restudied by Chen and Nisitani (1993), in which an explicit closed form expression was established for the singular stress field at the corner. Reedy and Guess (1997) analyzed the critical value of the stress singularity intensity at a wedge corner for a

* Corresponding author. Tel.: +65-799-4726; fax: +65-6791-1859.
E-mail address: mzxiao@ntu.edu.sg (Z.M. Xiao).

0020-7683/03/$ - see front matter © 2003 Elsevier Science Ltd. All rights reserved.
doi:10.1016/S0020-7683(03)00064-7

micro-crack to be initiated. Reedy (2000) further studied the connection between the failure criteria based on the critical values of singularity intensity factor at the wedge corner and the traditional stress intensity factor. Pahn and Earmme (2000) investigated the problem for a crack initiated from the corner of a rectangular inclusion. Xiao et al. (2001) obtained the elastic solutions for a single edge dislocation near a wedge-shaped bi-material interface, which can be used as the Green's function to study interaction problems for a crack near a wedge corner.

Recently, piezoelectric materials have become widely used in device applications such as sensors and actuators. Due to their intrinsic electro-mechanical coupling phenomenon, various types of defects embedded in piezoelectric materials, such as dislocations, cracks, cavities, and inclusions, can adversely influence the performance of such piezoelectric devices. Therefore, it is important to analyze the behavior of such defects under both electrical and mechanical loads. A number of research works on dislocations and cracks in piezoelectric solids have been published in open literature. To name a few, Deeg (1980) examined the effect of a dislocation, a crack and an inclusion upon the coupled response of piezoelectric solids. Pak (1990a) obtained closed form solutions for a screw dislocation in a piezoelectric solid subjected to external loads, he derived the generalized Peach-Koehler forces acting on the screw dislocation. Chung and Ting (1995) investigated a line dislocation at the apex of a piezoelectric composite wedges or spaces. Liu et al. (1999) studied the interaction between a screw dislocation and a piezoelectric bi-material interface. Lee et al. (2000) derived an exact solution for the interaction problem of a semi-infinite crack and a screw dislocation in a piezoelectric material. Chen et al. (2002) obtained an exact solution for the interaction problem of a semi-infinite anti-crack, a line force, a line charge and a line screw dislocation in a piezoelectric material.

In this paper, we focus on the interaction problem of a dislocation near a wedge-shaped bi-material interface. The materials are assumed to have piezoelectric behaviors. The present solution can be seen as an extension of our previous study (Xiao et al., 2001) where the piezoelectric behaviors have not been taken into account.

The objective of the present paper is to obtain the electro-elastic solution for a piezoelectric screw dislocation interacting with a nearby wedge-shaped bi-material interface as shown in Fig. 1. The dislocation is loaded by a line force and a line charge. The two materials are referred to as Material I and Material II. Without loss of generality, the dislocation $\mathbf{b} = (b_z, b_\varphi)$ with a line force p and a line charge q acted at its core is assumed to be located in Material I. Here b_φ is known as the electric-potential-dislocation.

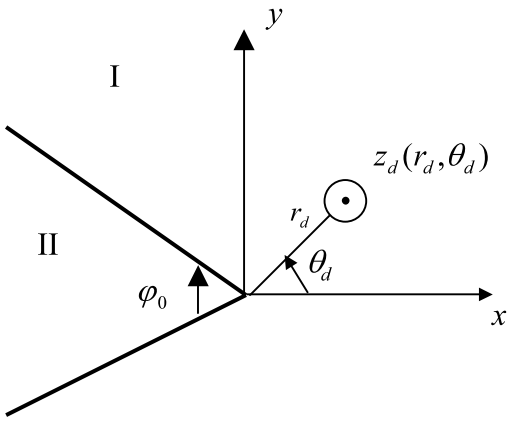

Fig. 1. A piezoelectric screw dislocation near a wedge-shaped inhomogeneity.

2. Basic formula

In a linear piezoelectric medium, the governing field equations and constitutive relations at constant temperature can be written as

$$\sigma_{ij,j} = 0, \tag{2.1a}$$

$$D_{i,i} = 0, \tag{2.1b}$$

$$\sigma_{ij} = c_{ijkl}u_{k,l} - e_{kij}E_k, \tag{2.2a}$$

$$D_i = e_{ikl}u_{k,l} + \varepsilon_{ik}E_k, \tag{2.2b}$$

where σ_{ij}, u_i, D_i and E_i are stress, displacement, electric displacement and electric fields, respectively. c_{ijkl}, e_{kij} and ε_{ij} are the corresponding elastic, piezoelectric and dielectric constants which satisfy the following relations

$$c_{ijkl} = c_{klij} = c_{ijlk} = c_{jikl}, \quad e_{kij} = e_{kji}, \quad \varepsilon_{ik} = \varepsilon_{ki}. \tag{2.3}$$

As the current problem is an anti-plane one, the anti-plane displacement w is coupled with the in-plane electric field E_x and E_y, where the variables are independent of the longitudinal coordinate z, such that

$$w = w(x,y), \quad E_x = E_x(x,y), \quad E_y = E_y(x,y). \tag{2.4}$$

The governing field equations and constitutive relations in (2.1) and (2.2) are reduced to

$$\frac{\partial \sigma_{zx}}{\partial x} + \frac{\partial \sigma_{zy}}{\partial y} = 0, \quad \frac{\partial D_x}{\partial x} + \frac{\partial D_y}{\partial y} = 0, \tag{2.5}$$

$$\sigma_{zx} = c_{44}\frac{\partial w}{\partial x} + e_{15}\frac{\partial \varphi}{\partial x}, \quad \sigma_{zy} = c_{44}\frac{\partial w}{\partial y} + e_{15}\frac{\partial \varphi}{\partial y}, \tag{2.6a}$$

$$D_x = e_{15}\frac{\partial w}{\partial x} - \varepsilon_{11}\frac{\partial \varphi}{\partial x}, \quad D_y = e_{15}\frac{\partial w}{\partial y} - \varepsilon_{11}\frac{\partial \varphi}{\partial y}, \tag{2.6b}$$

where $\varphi = \varphi(x,y)$ is the electric potential and

$$E_x = -\frac{\partial \varphi}{\partial x}, \quad E_y = -\frac{\partial \varphi}{\partial y}. \tag{2.7}$$

Substitution of (2.6) into (2.5) yields

$$c_{44}\nabla^2 w + e_{15}\nabla^2 \varphi = 0, \tag{2.8a}$$

$$e_{15}\nabla^2 w - \varepsilon_{11}\nabla^2 \varphi = 0, \tag{2.8b}$$

where ∇^2 is the two-dimensional Laplacian operator. The above equations can be satisfied if we choose

$$\nabla^2 \mathbf{u} = 0, \tag{2.9}$$

where

$$\mathbf{u} = \{w, \varphi\}^{\mathrm{T}} \tag{2.10}$$

is the generalized displacement vector.

From (2.10), the strain and electric fields can be expressed as

$$\boldsymbol{\varepsilon}_x = \{\gamma_{zx}, -E_x\}^{\mathrm{T}} = \frac{\partial \mathbf{u}}{\partial x}, \tag{2.11}$$

$$\boldsymbol{\varepsilon}_y = \{\gamma_{zy}, -E_y\}^{\mathrm{T}} = \frac{\partial \mathbf{u}}{\partial y}, \tag{2.12}$$

while the stress and electric displacement fields can be expressed as

$$\mathbf{t}_x = \{\sigma_{zx}, D_x\}^{\mathrm{T}} = \mathbf{C}\frac{\partial \mathbf{u}}{\partial x}, \tag{2.13}$$

$$\mathbf{t}_y = \{\sigma_{zy}, D_y\}^{\mathrm{T}} = \mathbf{C}\frac{\partial \mathbf{u}}{\partial y}, \tag{2.14}$$

with

$$\mathbf{C} = \begin{bmatrix} c_{44} & e_{15} \\ e_{15} & -\varepsilon_{11} \end{bmatrix}. \tag{2.15}$$

Eq. (2.9) indicates that $\mathbf{u}$ is a harmonic function vector which can be taken as the real part of some complex potentials of the complex variable $z = x + \mathrm{i}y = re^{\mathrm{i}\theta}$, such that

$$\mathbf{u} = \mathrm{Re}\{f_w(z), f_\varphi(z)\}^{\mathrm{T}} = \mathrm{Re}[\mathbf{f}(z)], \tag{2.16}$$

where Re stands for the real part. Then (2.11)–(2.14) can be combined as

$$\boldsymbol{\varepsilon}_x - \mathrm{i}\boldsymbol{\varepsilon}_y = \mathbf{f}'(z), \tag{2.17}$$

$$\mathbf{t}_x - \mathrm{i}\mathbf{t}_y = \mathbf{C}\mathbf{f}'(z), \tag{2.18}$$

where the prime denotes the derivative with respect to the argument z. Therefore, the resultant force and normal component of the electric displacement along any arbitrary arc AB is

$$\mathbf{T} = \int_A^B \mathbf{t}_x d_y - \mathbf{t}_y \,\mathrm{d}x = \mathbf{C}\,\mathrm{Im}[\mathbf{f}(z)]_A^B, \tag{2.19}$$

where Im stands for the imaginary part.

3. Solution of the problem

The bonding between Material I and Material II is assumed to be perfect, where the continuity conditions along the interface $\theta = \pm(\pi - \varphi_0/2)$ can be written as

$$\mathbf{u}^{(1)}(z) = \mathbf{u}^{(2)}(z), \qquad \mathbf{T}^{(1)}(z) = \mathbf{T}^{(2)}(z). \tag{3.1}$$

Inserting (2.16) and (2.19) into (3.1) yields

$$\mathrm{Re}[\mathbf{f}^{(1)}(z)] = \mathrm{Re}[\mathbf{f}^{(2)}(z)], \quad \mathbf{C}^{(1)}\mathrm{Im}[\mathbf{f}^{(1)}(z)] = \mathbf{C}^{(2)}\mathrm{Im}[\mathbf{f}^{(2)}(z)]. \tag{3.2}$$

Our next main task is to determine the complex potentials $\mathbf{f}^{(1)}(z)$ and $\mathbf{f}^{(2)}(z)$ by using (3.2) and the discontinuity conditions of elastic displacement and electric potential for a piezoelectric screw dislocation.

The complex potentials $\mathbf{f}^{(1)}(z)$ and $\mathbf{f}^{(2)}(z)$ can be written as

$$\mathbf{f}^{(1)}(z) = \mathbf{f}_0^{(1)}(z) + \mathbf{f}_1^{(1)}(z), \quad \mathbf{f}^{(2)}(z) = \mathbf{f}_1^{(2)}(z), \tag{3.3}$$

where $\mathbf{f}_0^{(1)}(z)$ is associated with the unperturbed field which is related to the solutions of an infinite homogeneous medium and is holomorphic in the entire domain except at z_d. The functions $\mathbf{f}_1^{(1)}(z)$ and $\mathbf{f}_1^{(2)}(z)$ are holomorphic and correspond to the perturbed fields in the domains occupied by Material I and Material II, respectively.

Introducing the mapping function

$$z = \varsigma^{1/\lambda}, \tag{3.4}$$

with $\lambda = \pi/(2\pi - \varphi_0)$ and $\varsigma = \xi + \mathrm{i}\eta$, it maps the boundary $\theta = \pm(\pi - \varphi_0/2)$ in the z-plane into the imaginary axis in the ς-plane as shown in Fig. 2. As a result, the continuity conditions along the interface in the ς-plane become

$$\mathbf{u}^{(1)}(\varsigma_c) = \mathbf{u}^{(2)}(\varsigma_c), \quad \mathbf{T}^{(1)}(\varsigma_c) = \mathbf{T}^{(2)}(\varsigma_c), \tag{3.5}$$

or

$$\mathrm{Re}[\mathbf{f}^{(1)}(\varsigma_c)] = \mathrm{Re}[\mathbf{f}^{(2)}(\varsigma_c)], \quad \mathbf{C}^{(1)}\mathrm{Im}[\mathbf{f}^{(1)}(\varsigma_c)] = \mathbf{C}^{(2)}\mathrm{Im}[\mathbf{f}^{(2)}(\varsigma_c)], \tag{3.6}$$

where ς_c is along the imaginary axis. Eq. (3.6) can be rewritten as

$$\mathbf{f}^{(1)}(\varsigma_c) + \overline{\mathbf{f}^{(1)}(\varsigma_c)} = \mathbf{f}^{(2)}(\varsigma_c) + \overline{\mathbf{f}^{(2)}(\varsigma_c)}, \tag{3.7a}$$

$$\mathbf{C}^{(1)}[\mathbf{f}^{(1)}(\varsigma_c) - \overline{\mathbf{f}^{(1)}(\varsigma_c)}] = \mathbf{C}^{(2)}[\mathbf{f}^{(2)}(\varsigma_c) - \overline{\mathbf{f}^{(2)}(\varsigma_c)}], \tag{3.7b}$$

where the over-bar denotes the complex conjugate.

Substituting (3.3) into (3.7), and noting that $\bar{\varsigma}_c = -\varsigma_c$ holds along the imaginary axis, we have

$$\mathbf{f}_0^{(1)}(\varsigma_c) + \overline{\mathbf{f}_1^{(1)}}(-\varsigma_c) - \mathbf{f}_1^{(2)}(\varsigma_c) = \overline{\mathbf{f}_1^{(2)}}(-\varsigma_c) - \overline{\mathbf{f}_0^{(1)}}(-\varsigma_c) - \mathbf{f}_1^{(1)}(\varsigma_c), \tag{3.8a}$$

$$\mathbf{C}^{(1)}\mathbf{f}_0^{(1)}(\varsigma_c) - \mathbf{C}^{(1)}\overline{\mathbf{f}_1^{(1)}}(-\varsigma_c) - \mathbf{C}^{(2)}\mathbf{f}_1^{(2)}(\varsigma_c) = \mathbf{C}^{(1)}\overline{\mathbf{f}_0^{(1)}}(-\varsigma_c) - \mathbf{C}^{(2)}\overline{\mathbf{f}_0^{(2)}}(-\varsigma_c) - \mathbf{C}^{(1)}\mathbf{f}_1^{(1)}(\varsigma_c), \tag{3.8b}$$

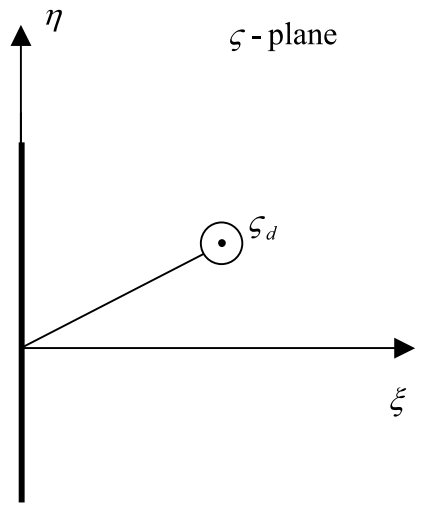

Fig. 2. A piezoelectric screw dislocation near a bi-material interface.

Using the standard analytic continuation arguments (Muskhelishvili, 1975), we obtain

$$\mathbf{f}_1^{(1)}(\varsigma) = (\mathbf{C}^{(1)} + \mathbf{C}^{(2)})^{-1}(\mathbf{C}^{(1)} - \mathbf{C}^{(2)})\bar{\mathbf{f}}_0^{(1)}(-\varsigma), \tag{3.9a}$$

$$\mathbf{f}_1^{(2)}(\varsigma) = 2(\mathbf{C}^{(1)} + \mathbf{C}^{(2)})^{-1}\mathbf{C}^{(1)}\mathbf{f}_0^{(1)}(\varsigma). \tag{3.9b}$$

Finally, the complex potential for the current problem in the ς plane is obtained as

$$\mathbf{f}^{(1)}(\varsigma) = \mathbf{f}_0^{(1)}(\varsigma) + (\mathbf{C}^{(1)} + \mathbf{C}^{(2)})^{-1}(\mathbf{C}^{(1)} - \mathbf{C}^{(2)})\bar{\mathbf{f}}_0^{(1)}(-\varsigma), \tag{3.10a}$$

$$\mathbf{f}^{(2)}(\varsigma) = 2(\mathbf{C}^{(1)} + \mathbf{C}^{(2)})^{-1}\mathbf{C}^{(1)}\mathbf{f}_0^{(1)}(\varsigma), \tag{3.10b}$$

where

$$\mathbf{f}_0^{(1)}(\varsigma) = \mathbf{A}^{(1)}\log(\zeta - \zeta_d), \tag{3.11}$$

with

$$\mathbf{A}^{(1)} = \left\{A_1^{(1)} + \mathrm{i}A_2^{(1)}, B_1^{(1)} + \mathrm{i}B_2^{(1)}\right\}^{\mathrm{T}}, \tag{3.12}$$

and

$$A_1^{(1)} = \frac{1}{2\pi}\frac{e_{15}^{(1)}q - \varepsilon_{11}^{(1)}p}{c_{44}^{(1)}\varepsilon_{11}^{(1)} + e_{15}^{(1)}e_{15}^{(1)}}, \quad A_2^{(1)} = -\frac{b_z}{2\pi}, \tag{3.13a}$$

$$B_1^{(1)} = -\frac{1}{2\pi}\frac{e_{15}^{(1)}p + c_{44}^{(1)}q}{{}^{(1)}_{44}\varepsilon_{11}^{(1)} + e_{15}^{(1)}e_{15}^{(1)}}, \quad B_2^{(1)} = -\frac{b_\varphi}{2\pi}, \tag{3.13b}$$

in which b_z, b_φ, p and q are the displacement discontinuity, electric potential across the slip plane, line force and line charge at the dislocation core, respectively.

By doing the reverse mapping, the complex potentials in the physical plane are obtained as

$$\mathbf{f}^{(1)}(z) = \mathbf{A}^{(1)}\log(z^\lambda - z_d^\lambda) + (\mathbf{C}^{(1)} + \mathbf{C}^{(2)})^{-1}(\mathbf{C}^{(1)} - \mathbf{C}^{(2)})\bar{\mathbf{A}}^{(1)}\log(z^\lambda + \bar{z}_d^\lambda), \tag{3.14a}$$

$$\mathbf{f}^{(2)}(z) = 2(\mathbf{C}^{(1)} + \mathbf{C}^{(2)})^{-1}\mathbf{C}^{(1)}\mathbf{A}^{(1)}\log(z^\lambda - z_d^\lambda), \tag{3.14b}$$

where

$$\bar{\mathbf{A}}^{(1)} = \{A_1^{(1)} - \mathrm{i}A_2^{(1)}, B_1^{(1)} - \mathrm{i}B_2^{(1)}\}^{\mathrm{T}}. \tag{3.15}$$

It is worth to note that when $\lambda = 1$, the solution is fully reduced to a dislocation in a straight piezoelectric bi-material interface. The detailed solution can be found in Liu et al. (1999).

4. Stress and electric displacement intensity factors (SEDIF)

As discussed in the Introduction, a wedge-shaped interface introduces a stress singularity at its corner where a micro-crack could be easily initiated. In this section, the stress and electric fields are found and the relative intensity factors are calculated. The strain, electric, stress and electric displacement fields are calculated using (2.17), (2.18) and (3.14) such that

$$\begin{bmatrix} \gamma_{zx}^{(1)} & \gamma_{zy}^{(1)} \\ -E_x^{(1)} & -E_y^{(1)} \end{bmatrix} = \begin{bmatrix} \gamma_{zx}^{0} & \gamma_{zy}^{0} \\ -E_x^{0} & -E_y^{0} \end{bmatrix} + \begin{bmatrix} a_{11}^{(1)} & a_{12}^{(1)} \\ a_{21}^{(1)} & a_{22}^{(1)} \end{bmatrix} \begin{bmatrix} \gamma_{zx}^{a} & \gamma_{zy}^{a} \\ -E_x^{a} & -E_y^{a} \end{bmatrix}, \tag{4.1}$$

$$\begin{bmatrix} \gamma_{zx}^{(2)} & \gamma_{zy}^{(2)} \\ -E_x^{(2)} & -E_y^{(2)} \end{bmatrix} = \begin{bmatrix} a_{11}^{(2)} & a_{12}^{(2)} \\ a_{21}^{(2)} & a_{22}^{(2)} \end{bmatrix} \begin{bmatrix} \gamma_{zx}^{0} & \gamma_{zy}^{0} \\ -E_x^{0} & -E_y^{0} \end{bmatrix}, \tag{4.2}$$

$$\begin{bmatrix} \sigma_{zx}^{(1)} & \sigma_{zy}^{(1)} \\ D_x^{(1)} & D_y^{(1)} \end{bmatrix} = \begin{bmatrix} \sigma_{zx}^{0} & \sigma_{zy}^{0} \\ D_x^{0} & D_y^{0} \end{bmatrix} + \begin{bmatrix} b_{11}^{(1)} & b_{12}^{(1)} \\ b_{21}^{(1)} & b_{22}^{(1)} \end{bmatrix} \begin{bmatrix} \sigma_{zx}^{a} & \sigma_{zy}^{a} \\ D_x^{a} & D_y^{a} \end{bmatrix}, \tag{4.3}$$

$$\begin{bmatrix} \sigma_{zx}^{(2)} & \sigma_{zy}^{(2)} \\ D_x^{(2)} & D_y^{(2)} \end{bmatrix} = \begin{bmatrix} b_{11}^{(2)} & b_{12}^{(2)} \\ b_{21}^{(2)} & b_{22}^{(2)} \end{bmatrix} \begin{bmatrix} \sigma_{zx}^{0} & \sigma_{zy}^{0} \\ D_x^{0} & D_y^{0} \end{bmatrix}, \tag{4.4}$$

where the matrices on the right-hand side of the equation are listed in Appendix A. Both the stress and electric displacement show $r^{\lambda-1}(1/2 \leqslant \lambda \leqslant 1)$ type of singularity near the tip of the wedge. If we define an intensity factor vector induced by the dislocation as

$$\mathbf{K}_{\mathrm{D}} = \begin{bmatrix} K_{\sigma_{zx}} - \mathrm{i}K_{\sigma_{zy}} \\ K_{\mathrm{D}_x} - \mathrm{i}K_{\mathrm{D}_y} \end{bmatrix}, \tag{4.5}$$

then,

$$\mathbf{K}_{\mathrm{D}} = \lim_{z->0} (2\pi z)^{1-\lambda} \left[\mathbf{C}^{(1)} \frac{\mathrm{d}\mathbf{f}^{(1)}(z)}{\mathrm{d}z} \right]. \tag{4.6}$$

Substituting (3.14a) into the above equation, we obtain

$$\mathbf{K}_{\mathrm{D}} = -\lambda(2\pi)^{1-\lambda} \{ \mathbf{C}^{(1)} \mathbf{A}^{(1)} z_d^{-\lambda} - \mathbf{C}^{(1)} (\mathbf{C}^{(1)} + \mathbf{C}^{(2)})^{-1} (\mathbf{C}^{(1)} - \mathbf{C}^{(2)}) \bar{\mathbf{A}}^{(1)} \bar{z}_d^{-\lambda} \}. \tag{4.7}$$

5. Image force on the dislocation

One of the major interests is calculating the image force acting on the dislocation. Following Pak (1990a), the generalized Peach Koehler forces acting on a screw dislocation with a line force and a line charge can be written as

$$F_x = b_z \sigma_{zy}^{\mathrm{T}} + b_\phi D_y^{\mathrm{T}} + p\gamma_{zx}^{\mathrm{T}} + qE_x^{\mathrm{T}}, \tag{5.1}$$

$$F_y = -b_z \sigma_{zx}^{\mathrm{T}} - b_\phi D_x^{\mathrm{T}} + p\gamma_{zy}^{\mathrm{T}} + qE_y^{\mathrm{T}}, \tag{5.2}$$

where the variables σ_{zy}^{T}, σ_{zx}^{T}, D_y^{T}, D_x^{T}, γ_{zy}^{T}, γ_{zx}^{T}, E_y^{T} and E_x^{T} are calculated from

$$\begin{bmatrix} \gamma_{zx}^{\mathrm{T}} - \mathrm{i}\gamma_{zx}^{\mathrm{T}} \\ -E_x^{\mathrm{T}} + \mathrm{i}E_y^{\mathrm{T}} \end{bmatrix} = \boldsymbol{\varepsilon}_0 + (\mathbf{C}^{(1)} + \mathbf{C}^{(2)})^{-1} (\mathbf{C}^{(1)} - \mathbf{C}^{(2)}) \boldsymbol{\varepsilon}_1, \tag{5.3}$$

$$\begin{bmatrix} \sigma_{zx}^{\mathrm{T}} & \sigma_{zx}^{\mathrm{T}} \\ D_x^{\mathrm{T}} & D_x^{\mathrm{T}} \end{bmatrix} = \begin{bmatrix} c_{44}^{(1)} & e_{15}^{(1)} \\ e_{15}^{(1)} & -\varepsilon_{11}^{(1)} \end{bmatrix} \begin{bmatrix} \gamma_{zx}^{\mathrm{T}} & \gamma_{zx}^{\mathrm{T}} \\ -E_x^{\mathrm{T}} & -E_x^{\mathrm{T}} \end{bmatrix}, \tag{5.4}$$

with

$$\boldsymbol{\varepsilon}_0 = \frac{\lambda - 1}{2z_d} \mathbf{A}^{(1)}, \tag{5.5}$$

$$\boldsymbol{\varepsilon}_1 = \frac{\lambda z_d^{\lambda-1}}{z_d^{\lambda} + \bar{z}_d^{\lambda}} \bar{\mathbf{A}}^{(1)}. \tag{5.6}$$

So that we have

$$\begin{bmatrix} \gamma_{zx}^{\mathrm{T}} & \gamma_{zy}^{\mathrm{T}} \\ -E_x^{\mathrm{T}} & -E_y^{\mathrm{T}} \end{bmatrix} = \begin{bmatrix} \gamma_{zx}^{\mathrm{T0}} & \gamma_{zy}^{\mathrm{T0}} \\ -E_x^{\mathrm{T0}} & -E_y^{\mathrm{T0}} \end{bmatrix} + \begin{bmatrix} a_{11}^{(1)} & a_{12}^{(1)} \\ a_{21}^{(1)} & a_{22}^{(1)} \end{bmatrix} \begin{bmatrix} \gamma_{zx}^{\mathrm{T}a} & \gamma_{zy}^{\mathrm{T}a} \\ -E_x^{\mathrm{T}a} & -E_y^{\mathrm{T}a} \end{bmatrix}, \tag{5.7}$$

$$\begin{bmatrix} \sigma_{zx}^{\mathrm{T}} & \sigma_{zy}^{\mathrm{T}} \\ D_x^{\mathrm{T}} & D_y^{\mathrm{T}} \end{bmatrix} = \begin{bmatrix} \sigma_{zx}^{\mathrm{T0}} & \sigma_{zy}^{\mathrm{T0}} \\ D_x^{\mathrm{T0}} & D_y^{0} \end{bmatrix} + \begin{bmatrix} b_{11}^{(1)} & b_{12}^{(1)} \\ b_{21}^{(1)} & b_{22}^{(1)} \end{bmatrix} \begin{bmatrix} \sigma_{zx}^{\mathrm{T}a} & \sigma_{zy}^{\mathrm{T}a} \\ D_x^{\mathrm{T}a} & D_y^{\mathrm{T}a} \end{bmatrix}, \tag{5.8}$$

where the matrices on the right-hand side of the equation are listed in Appendix B. The radial and tangential components of the force on the dislocation can be calculated from

$$F_r = F_x \cos\theta_d + F_y \sin\theta_d, \tag{5.9}$$

$$F_t = -F_x \sin\theta_d + F_y \cos\theta_d. \tag{5.10}$$

6. Numerical examples and discussions

Eqs. (5.9) and (5.10) give the explicit expressions for the force on the dislocation due to a screw dislocation (b_z, b_φ), a line charge (q) and a line force (p) located at (r_d, θ_d) in a wedge-shaped piezoelectric bimaterial. In our solutions, the wedge angle α_0 can be any value with any material property. In order to have a better understanding on the engineering applications of the current problem, examples with some particular values of angle α_0 and material property combinations are given in the following sub-sections. In our numerical calculations, we assume$p = q = 0$. The force on the dislocation is normalized by

$$F_z^0 = \frac{c_{44}^{(1)} b_z^2}{4\pi r_d}, \tag{6.1}$$

for b_z, and

$$F_\varphi^0 = \frac{\varepsilon_{11}^{(1)} b_\varphi^2}{4\pi r_d}, \tag{6.2}$$

for b_φ. Furthermore, we use the electric-mechanical coupling factor

$$k = \sqrt{e_{15}^{(1)} e_{15}^{(1)} / c_{44}^{(1)} \varepsilon_{11}^{(1)}}. \tag{6.3}$$

To characterize the piezoelectric strength of Material I, three material constant ratios are introduced as

$$c = c_{44}^{(2)} / c_{44}^{(1)}, \tag{6.4}$$

$$\varepsilon = \varepsilon_{11}^{(2)} / \varepsilon_{11}^{(1)}, \tag{6.5}$$

$$e = e_{15}^{(2)} / e_{15}^{(1)}. \tag{6.6}$$

Then, the normalized radial and tangential components of the image force on the dislocation b_z and b_φ can be expressed in terms of the dimensionless parameters c, e, k and ε as

$$F^*_{rb_z} = \frac{-(1+c+\varepsilon+c\varepsilon+k^2+2ek^2+e^2k^2)+\lambda(2c+2c\varepsilon+2k^2c+2e^2k^2)}{1+\varepsilon+c+c\varepsilon+k^2+2ek^2+e^2k^2}, \tag{6.7}$$

$$F^*_{tb_z} = \frac{\lambda(1+\varepsilon-c-c\varepsilon+k^2-2k^2c+2ek^2-e^2k^2)\tan\theta_d}{1+\varepsilon+c+c\varepsilon+k^2+2ek^2+e^2k^2}, \tag{6.8}$$

$$F^*_{rb_\varphi} = \frac{1+\varepsilon+c+c\varepsilon+k^2+2ek^2+e^2k^2-\lambda(2\varepsilon+2c\varepsilon+2k^2\varepsilon+2e^2k^2)}{1+\varepsilon+c+c\varepsilon+k^2+2ek^2+e^2k^2}, \tag{6.9}$$

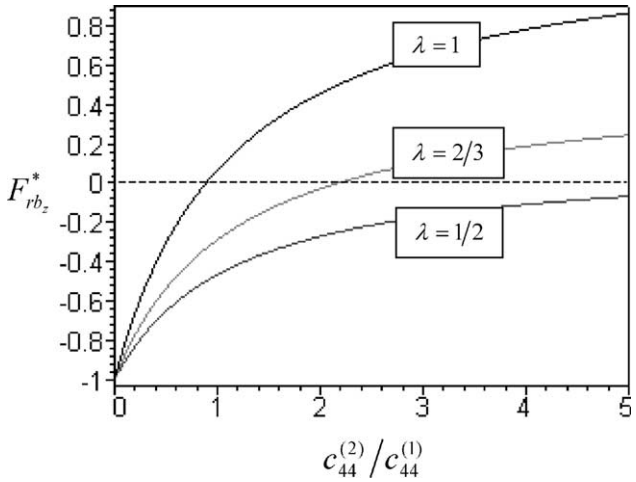

Fig. 3. $F^*_{rb_z}$ versus $c = c^{(2)}_{44}/c^{(1)}_{44}$ with $k = 0.542$, $\varepsilon^{(2)}_{11}/\varepsilon^{(1)}_{11} = 1$, $e^{(2)}_{15}/e^{(1)}_{15} = 0$.

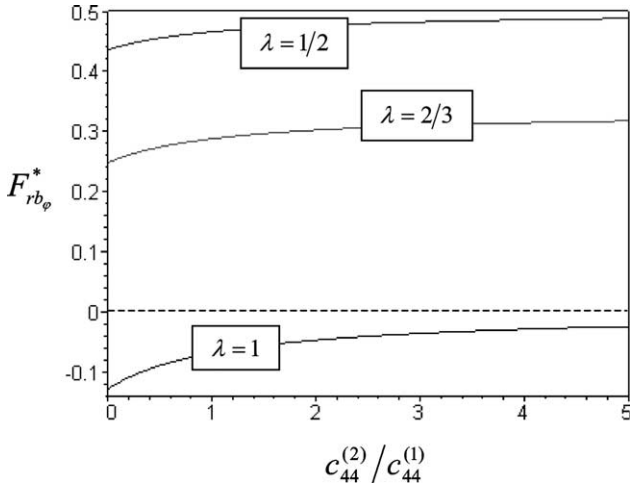

Fig. 4. $F^*_{rb_\varphi}$ versus $c = c^{(2)}_{44}/c^{(1)}_{44}$ with $k = 0.542$, $\varepsilon^{(2)}_{11}/\varepsilon^{(1)}_{11} = 1$, $e^{(2)}_{15}/e^{(1)}_{15} = 0$.

and

$$F^*_{tb_\varphi} = \frac{\lambda(e^2k^2 - 2ek^2 + 2k^2\varepsilon - k^2 + c\varepsilon + \varepsilon - c - 1)\tan\theta_d}{1 + \varepsilon + c + c\varepsilon + k^2 + 2ek^2 + e^2k^2}, \tag{6.10}$$

where $F^*_{rb_z}$, $F^*_{tb_z}$ are named as normalized radial and tangential components of the force on the dislocation b_z when $b_\varphi = 0$, respectively; while $F^*_{rb_\varphi}$, $F^*_{tb_\varphi}$ are normalized radial and tangential components of the force on the dislocation b_φ when $b_z = 0$, respectively.

It is apparent to conclude from Eqs. (6.7)–(6.10) that the radial components of the force on the dislocation are independent of θ_d, whilst the tangential components are closely related to $\tan\theta_d$.

The forces $F^*_{rb_z}$ and $F^*_{rb_\varphi}$ versus $c = c^{(2)}_{44}/c^{(1)}_{44}$ for different wedge angles are depicted in Figs. 3 and 4 respectively for $\lambda = 1$, $\lambda = 2/3$, $\lambda = 1/2$ and $\varepsilon^{(2)}_{11}/\varepsilon^{(1)}_{11} = 1$. Material I is taken to be PZT-5H piezoelectric ceramic with $k = 0.542$ (Pak, 1990b), and Material II is assumed to be pure elastic $e^{(2)}_{15} = 0$. Here $\lambda = 1$

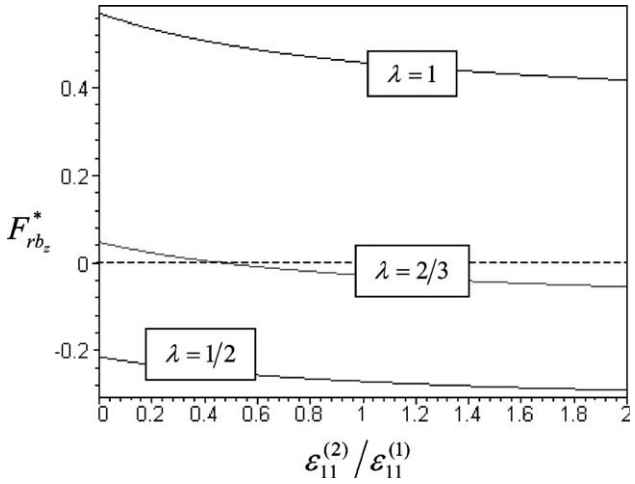

Fig. 5. $F^*_{rb_z}$ versus $\varepsilon = \varepsilon^{(2)}_{11}/\varepsilon^{(1)}_{11}$ with $k = 0.542$, $c^{(2)}_{44}/c^{(1)}_{44} = 2$, $e^{(2)}_{15}/e^{(1)}_{15} = 0$.

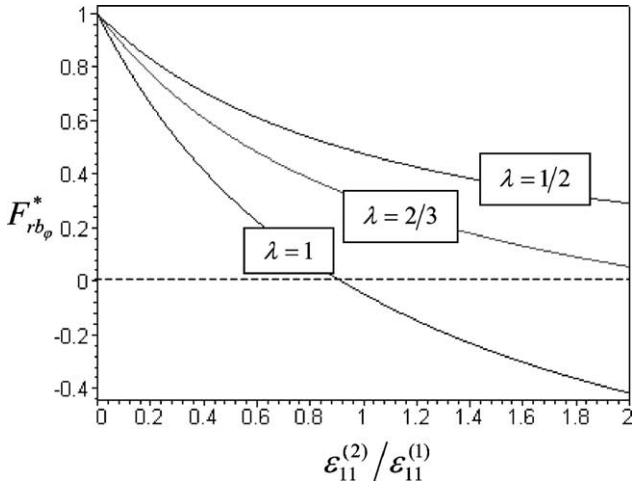

Fig. 6. $F^*_{rb_\varphi}$ versus $\varepsilon = \varepsilon^{(2)}_{11}/\varepsilon^{(1)}_{11}$ with $k = 0.542$, $c^{(2)}_{44}/c^{(1)}_{44} = 2$, $e^{(2)}_{15}/e^{(1)}_{15} = 0$.

represents a straight interface, $\lambda = 2/3$ is a rectangular inhomogeneity case and $\lambda = 1/2$ is for a line inhomogeneity case. Fig. 3 indicates that the elastic constant of Material II affects the radial component of the force to a different extent at different wedge angles. For the straight interface case ($\lambda = 1$), $F^*_{rb_z}$ changes its direction around $c_{cr} = c^{(2)}_{44}/c^{(1)}_{44} = 1$. The value of c_{cr} increases with decreasing the wedge angle. When the wedge angle becomes zero (the line inhomogeneity case ($\lambda = 1/2$)), $F^*_{rb_z}$ never changes its direction. However, the elastic constant of Material II has little influence on the force of the electric-potential dislocation$F^*_{rb_\varphi}$, also this force never changes its direction, as shown in Fig. 4.

The influence from the dielectric constant ratio $\varepsilon = \varepsilon^{(2)}_{11}/\varepsilon^{(1)}_{11}$ on normalized forces $F^*_{rb_z}$ and $F^*_{rb_\varphi}$ are plotted in Figs. 5 and 6 respectively with $k = 0.542$, $e = 0$ and $c^{(2)}_{44}/c^{(1)}_{44} = 2$ for $\lambda = 1$, $\lambda = 2/3$ and $\lambda = 1/2$. It is observed from these two figures that the dielectric constant of Material II has little effect on the force on the dislocation b_z; however, its influence on the electric-potential dislocation b_φ is significant. The direction of

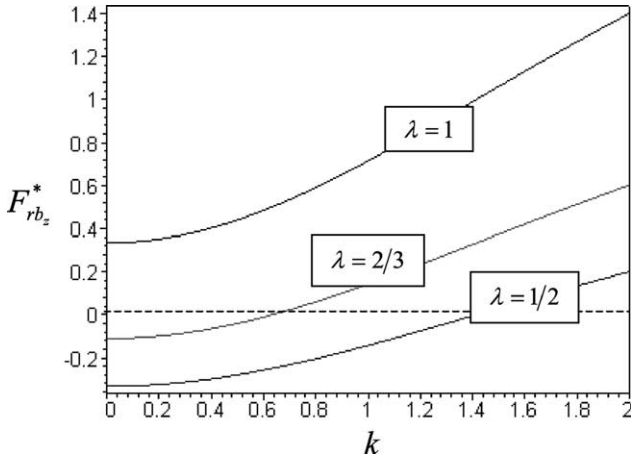

Fig. 7. $F^*_{rb_z}$ versus k with $c^{(2)}_{44}/c^{(1)}_{44} = 2$, $\varepsilon^{(2)}_{11}/\varepsilon^{(1)}_{11} = 1$, $e^{(2)}_{15}/e^{(1)}_{15} = 0$.

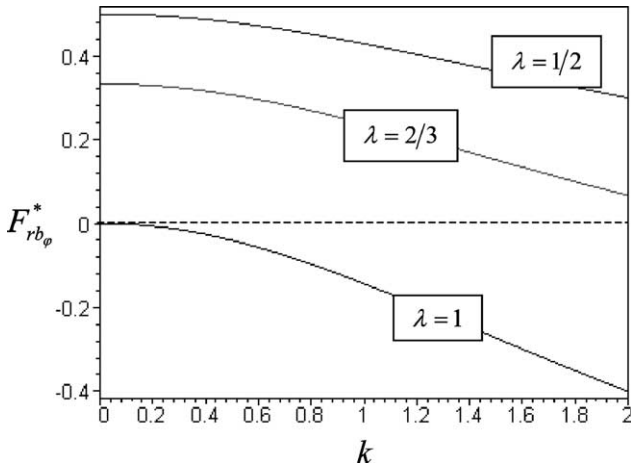

Fig. 8. $F^*_{rb_\varphi}$ versus k with $c^{(2)}_{44}/c^{(1)}_{44} = 2$, $\varepsilon^{(2)}_{11}/\varepsilon^{(1)}_{11} = 1$, $e^{(2)}_{15}/e^{(1)}_{15} = 0$.

force $F^*_{rb_\varphi}$ depends heavily on the value of $\varepsilon^{(2)}_{11}/\varepsilon^{(1)}_{11}$ when the wedge angle is large (e.g. $\lambda = 1$) as depicted in Fig. 6.

Figs. 7 and 8 show how the piezoelectric strength of Material I affects the force on the dislocation $F^*_{rb_z}$ and $F^*_{rb_\varphi}$ with $c^{(2)}_{44}/c^{(1)}_{44} = 2$, $e = 0$, $\varepsilon^{(2)}_{11}/\varepsilon^{(1)}_{11} = 1$ for $\lambda = 1$, $\lambda = 2/3$ and $\lambda = 1/2$. The piezoelectric strength of Material I enhances the force on the dislocation in the positive radial direction and reduces it in the negative radial direction. The bigger the k value, the stronger the image force in the positive radial direction.

The variations of normalized image forces $F^*_{rb_z}$ and $F^*_{rb_\varphi}$ versus the piezoelectric constant ratio $e = e^{(2)}_{15}/e^{(1)}_{15}$ are shown in Figs. 9 and 10 respectively, for three different wedge angles and $c^{(2)}_{44}/c^{(1)}_{44} = 0.2$, $\varepsilon^{(2)}_{11}/\varepsilon^{(1)}_{11} = 1$. Material I is taken as PZT-6B piezoelectric ceramic with $k = 0.271$. In the figure, $e = e^{(2)}_{15}/e^{(1)}_{15} < 0$ indicates that the poling directions of the two piezoelectric materials are opposite. It is observed that the parameters

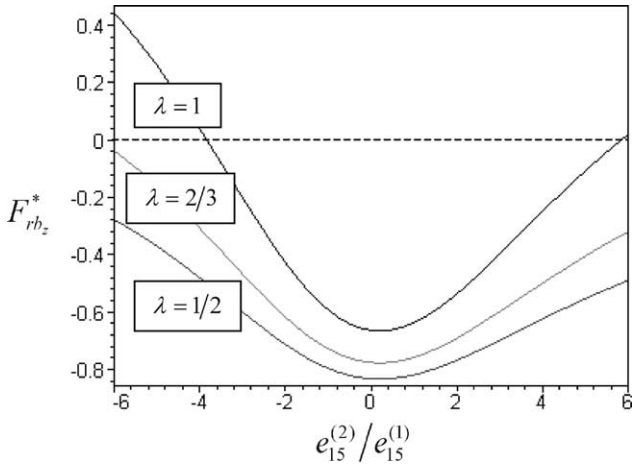

Fig. 9. $F^*_{rb_z}$ versus $e = e^{(2)}_{15}/e^{(1)}_{15}$ with $c^{(2)}_{44}/c^{(1)}_{44} = 0.2$, $\varepsilon^{(2)}_{11}/\varepsilon^{(1)}_{11} = 1$, $k = 0.271$.

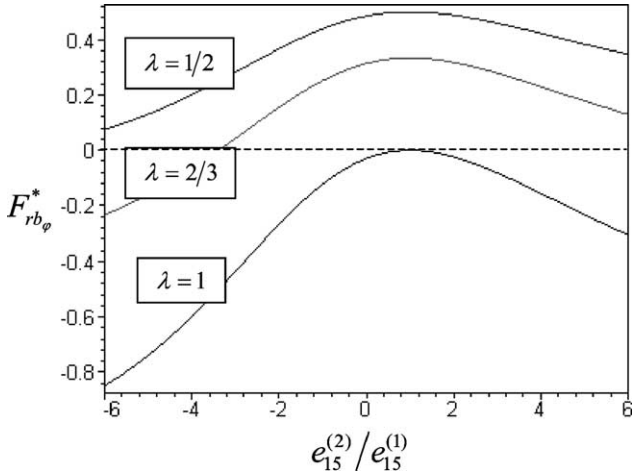

Fig. 10. $F^*_{rb_\varphi}$ versus $e = e^{(2)}_{15}/e^{(1)}_{15}$ with $c^{(2)}_{44}/c^{(1)}_{44} = 0.2$, $\varepsilon^{(2)}_{11}/\varepsilon^{(1)}_{11} = 1$, $k = 0.271$.

such as the wedge angle, the elastic moduli and the piezoelectric constant will all affect the sign of the image force in the radial direction.

7. Conclusions

In the current work, a line dislocation, a line force and a line charge in a wedge-shaped piezoelectric bimaterial structure are studied. Closed form solutions are derived for the stress, strain, electric displacement and electric fields in terms of complex potentials and their derivatives by using the complex variable method. The stress and electric displacement intensity factors and the image forces on the dislocation are calculated. Numerical examples for a straight interface, a rectangle and a line inhomogeneity are given to illustrate the influences of material constants, and piezoelectric strength on the image force.

Appendix A

$$\begin{bmatrix} a_{11}^{(1)} & a_{12}^{(1)} \\ a_{21}^{(1)} & a_{22}^{(1)} \end{bmatrix} = \begin{bmatrix} c_{44}^{(1)} + c_{44}^{(2)} & e_{15}^{(1)} + e_{15}^{(2)} \\ e_{15}^{(1)} + e_{15}^{(2)} & -\varepsilon_{11}^{(1)} - \varepsilon_{11}^{(2)} \end{bmatrix}^{-1} \begin{bmatrix} c_{44}^{(1)} - c_{44}^{(2)} & e_{15}^{(1)} - e_{15}^{(2)} \\ e_{15}^{(1)} - e_{15}^{(2)} & \varepsilon_{11}^{(2)} - \varepsilon_{11}^{(1)} \end{bmatrix}, \tag{A.1}$$

$$\begin{bmatrix} a_{11}^{(2)} & a_{12}^{(2)} \\ a_{21}^{(2)} & a_{22}^{(2)} \end{bmatrix} = 2 \begin{bmatrix} c_{44}^{(1)} + c_{44}^{(2)} & e_{15}^{(1)} + e_{15}^{(2)} \\ e_{15}^{(1)} + e_{15}^{(2)} & -\varepsilon_{11}^{(1)} - \varepsilon_{11}^{(2)} \end{bmatrix}^{-1} \begin{bmatrix} c_{44}^{(1)} & e_{15}^{(1)} \\ e_{15}^{(1)} & -\varepsilon_{11}^{(1)} \end{bmatrix}, \tag{A.2}$$

$$\begin{bmatrix} b_{11}^{(1)} & b_{12}^{(1)} \\ b_{21}^{(1)} & b_{22}^{(1)} \end{bmatrix} = \begin{bmatrix} c_{44}^{(1)} & e_{15}^{(1)} \\ e_{15}^{(1)} & -\varepsilon_{11}^{(1)} \end{bmatrix} \begin{bmatrix} a_{11}^{(1)} & a_{12}^{(1)} \\ a_{21}^{(1)} & a_{22}^{(1)} \end{bmatrix} \begin{bmatrix} c_{44}^{(1)} & e_{15}^{(1)} \\ e_{15}^{(1)} & -\varepsilon_{11}^{(1)} \end{bmatrix}^{-1}, \tag{A.3}$$

$$\begin{bmatrix} b_{11}^{(2)} & b_{12}^{(2)} \\ b_{21}^{(2)} & b_{22}^{(2)} \end{bmatrix} = \begin{bmatrix} c_{44}^{(2)} & e_{15}^{(2)} \\ e_{15}^{(2)} & -\varepsilon_{11}^{(2)} \end{bmatrix} \begin{bmatrix} a_{11}^{(2)} & a_{12}^{(2)} \\ a_{21}^{(2)} & a_{22}^{(2)} \end{bmatrix} \begin{bmatrix} c_{44}^{(1)} & e_{15}^{(1)} \\ e_{15}^{(1)} & -\varepsilon_{11}^{(1)} \end{bmatrix}^{-1}, \tag{A.4}$$

$$\gamma_{zx}^{0} = \frac{\lambda}{2\pi} \frac{e_{15}^{(1)} q - \varepsilon_{11}^{(1)} p}{c_{44}^{(1)} \varepsilon_{11} + e_{15}^{(1)} e_{15}^{(1)}} \frac{r^{2\lambda-1} \cos\theta - r^{\lambda-1} r_d^{\lambda} \cos[(1-\lambda)\theta + \lambda\theta_d]}{r^{2\lambda} + r_d^{2\lambda} - 2r^{\lambda} r_d^{\lambda} \cos\lambda(\theta - \theta_d)} - \frac{\lambda b_z}{2\pi} \frac{r^{2\lambda-1} \sin\theta - r^{\lambda-1} r_d^{\lambda} \sin[(1-\lambda)\theta + \lambda\theta_d]}{r^{2\lambda} + r_d^{2\lambda} - 2r^{\lambda} r_d^{\lambda} \cos\lambda(\theta - \theta_d)}, \tag{A.5}$$

$$\gamma_{zy}^{0} = \frac{\lambda}{2\pi} \frac{e_{15}^{(1)} q - \varepsilon_{11}^{(1)} p}{c_{44}^{(1)} \varepsilon_{11} + e_{15}^{(1)} e_{15}^{(1)}} \frac{r^{2\lambda-1} \sin\theta - r^{\lambda-1} r_d^{\lambda} \sin[(1-\lambda)\theta + \lambda\theta_d]}{r^{2\lambda} + r_d^{2\lambda} - 2r^{\lambda} r_d^{\lambda} \cos\lambda(\theta - \theta_d)} + \frac{\lambda b_z}{2\pi} \frac{r^{2\lambda-1} \cos\theta - r^{\lambda-1} r_d^{\lambda} \cos[(1-\lambda)\theta + \lambda\theta_d]}{r^{2\lambda} + r_d^{2\lambda} - 2r^{\lambda} r_d^{\lambda} \cos\lambda(\theta - \theta_d)}, \tag{A.6}$$

$$E_x^{0} = \frac{\lambda}{2\pi} \frac{e_{15}^{(1)} p + c_{44}^{(1)} q}{c_{44}^{(1)} \varepsilon_{11} + e_{15}^{(1)} e_{15}^{(1)}} \frac{r^{2\lambda-1} \cos\theta - r^{\lambda-1} r_d^{\lambda} \cos[(1-\lambda)\theta + \lambda\theta_d]}{r^{2\lambda} + r_d^{2\lambda} - 2r^{\lambda} r_d^{\lambda} \cos\lambda(\theta - \theta_d)} + \frac{\lambda b_{\varphi}}{2\pi} \frac{r^{2\lambda-1} \sin\theta - r^{\lambda-1} r_d^{\lambda} \sin[(1-\lambda)\theta + \lambda\theta_d]}{r^{2\lambda} + r_d^{2\lambda} - 2r^{\lambda} r_d^{\lambda} \cos\lambda(\theta - \theta_d)}, \tag{A.7}$$

$$E_y^0 = \frac{1}{2\pi}\frac{e_{15}^{(1)}p + c_{44}^{(1)}q}{c_{44}^{(1)}\varepsilon_{11} + e_{15}^{(1)}e_{15}^{(1)}}\frac{r^{2\lambda-1}\sin\theta - r^{\lambda-1}r_d^{\lambda}\sin[(1-\lambda)\theta + \lambda\theta_d]}{r^{2\lambda} + r_d^{2\lambda} - 2r^{\lambda}r_d^{\lambda}\cos\lambda(\theta - \theta_d)}$$
$$- \frac{\lambda b_\varphi}{2\pi}\frac{r^{2\lambda-1}\cos\theta - r^{\lambda-1}r_d^{\lambda}\cos[(1-\lambda)\theta + \lambda\theta_d]}{r^{2\lambda} + r_d^{2\lambda} - 2r^{\lambda}r_d^{\lambda}\cos\lambda(\theta - \theta_d)}, \tag{A.8}$$

$$\gamma_{zx}^a = \frac{\lambda}{2\pi}\frac{e_{15}^{(1)}q - \varepsilon_{11}^{(1)}p}{c_{44}^{(1)}\varepsilon_{11} + e_{15}^{(1)}e_{15}^{(1)}}\frac{r^{2\lambda-1}\cos\theta + r^{\lambda-1}r_d^{\lambda}\cos[(1-\lambda)\theta - \lambda\theta_d]}{r^{2\lambda} + r_d^{2\lambda} + 2r^{\lambda}r_d^{\lambda}\cos\lambda(\theta + \theta_d)}$$
$$+ \frac{\lambda b_z}{2\pi}\frac{r^{2\lambda-1}\sin\theta + r^{\lambda-1}r_d^{\lambda}\sin[(1-\lambda)\theta - \lambda\theta_d]}{r^{2\lambda} + r_d^{2\lambda} + 2r^{\lambda}r_d^{\lambda}\cos\lambda(\theta + \theta_d)}, \tag{A.9}$$

$$\gamma_{zy}^a = \frac{\lambda}{2\pi}\frac{e_{15}^{(1)}q - \varepsilon_{11}^{(1)}p}{c_{44}^{(1)}\varepsilon_{11} + e_{15}^{(1)}e_{15}^{(1)}}\frac{r^{2\lambda-1}\sin\theta - r^{\lambda-1}r_d^{\lambda}\sin[(\lambda-1)\theta + \lambda\theta_d]}{r^{2\lambda} + r_d^{2\lambda} + 2r^{\lambda}r_d^{\lambda}\cos\lambda(\theta + \theta_d)}$$
$$- \frac{\lambda b_z}{2\pi}\frac{r^{2\lambda-1}\cos\theta + r^{\lambda-1}r_d^{\lambda}\cos[(\lambda-1)\theta + \lambda\theta_d]}{r^{2\lambda} + r_d^{2\lambda} + 2r^{\lambda}r_d^{\lambda}\cos\lambda(\theta + \theta_d)}, \tag{A.10}$$

$$E_x^a = \frac{\lambda}{2\pi}\frac{e_{15}^{(1)}p + c_{44}^{(1)}q}{c_{44}^{(1)}\varepsilon_{11} + e_{15}^{(1)}e_{15}^{(1)}}\frac{r^{2\lambda-1}\cos\theta + r^{\lambda-1}r_d^{\lambda}\cos[(\lambda-1)\theta + \lambda\theta_d]}{r^{2\lambda} + r_d^{2\lambda} + 2r^{\lambda}r_d^{\lambda}\cos\lambda(\theta + \theta_d)}$$
$$- \frac{\lambda b_\varphi}{2\pi}\frac{r^{2\lambda-1}\sin\theta - r^{\lambda-1}r_d^{\lambda}\sin[(\lambda-1)\theta + \lambda\theta_d]}{r^{2\lambda} + r_d^{2\lambda} + 2r^{\lambda}r_d^{\lambda}\cos\lambda(\theta + \theta_d)}, \tag{A.11}$$

$$E_y^a = \frac{1}{2\pi}\frac{e_{15}^{(1)}p + c_{44}^{(1)}q}{c_{44}^{(1)}\varepsilon_{11} + e_{15}^{(1)}e_{15}^{(1)}}\frac{r^{2\lambda-1}\sin\theta - r^{\lambda-1}r_d^{\lambda}\sin[(\lambda-1)\theta + \lambda\theta_d]}{r^{2\lambda} + r_d^{2\lambda} + 2r^{\lambda}r_d^{\lambda}\cos\lambda(\theta + \theta_d)}$$
$$+ \frac{\lambda b_\varphi}{2\pi}\frac{r^{2\lambda-1}\cos\theta + r^{\lambda-1}r_d^{\lambda}\cos[(\lambda-1)\theta + \lambda\theta_d]}{r^{2\lambda} + r_d^{2\lambda} + 2r^{\lambda}r_d^{\lambda}\cos\lambda(\theta + \theta_d)}, \tag{A.12}$$

$$\begin{bmatrix}\sigma_{zx}^0 & \sigma_{zy}^0\\ D_x^0 & D_y^0\end{bmatrix} = \begin{bmatrix}c_{44}^{(1)} & e_{15}^{(1)}\\ e_{15}^{(1)} & -\varepsilon_{11}^{(1)}\end{bmatrix}\begin{bmatrix}\gamma_{zx}^0 & \gamma_{zy}^0\\ -E_x^0 & -E_y^0\end{bmatrix}, \tag{A.13}$$

$$\begin{bmatrix}\sigma_{zx}^a & \sigma_{zy}^a\\ D_x^a & D_y^a\end{bmatrix} = \begin{bmatrix}c_{44}^{(1)} & e_{15}^{(1)}\\ e_{15}^{(1)} & -\varepsilon_{11}^{(1)}\end{bmatrix}\begin{bmatrix}\gamma_{zx}^a & \gamma_{zy}^a\\ -E_x^a & -E_y^a\end{bmatrix}. \tag{A.14}$$

Appendix B

$$\gamma_{zx}^{T0} = \frac{\lambda - 1}{4\pi r_d}\left[\frac{e_{15}^{(1)}q - \varepsilon_{11}^{(1)}p}{c_{44}^{(1)}\varepsilon_{11}^{(1)} + e_{15}^{(1)}e_{15}^{(1)}}\cos\theta_d - b_z\sin\theta_d\right], \tag{B.1}$$

$$\gamma_{zy}^{T0} = \frac{\lambda - 1}{4\pi r_d}\left[\frac{e_{15}^{(1)}q - \varepsilon_{11}^{(1)}p}{c_{44}^{(1)}\varepsilon_{11}^{(1)} + e_{15}^{(1)}e_{15}^{(1)}}\sin\theta_d + b_z\cos\theta_d\right], \tag{B.2}$$

$$E_x^{T0} = \frac{\lambda - 1}{4\pi r_d}\left[\frac{e_{15}^{(1)} p + c_{44}^{(1)} q}{c_{44}^{(1)}\varepsilon_{11}^{(1)} + e_{15}^{(1)} e_{15}^{(1)}}\cos\theta_d + b_\varphi \sin\theta_d\right], \tag{B.3}$$

$$E_y^{T0} = \frac{\lambda - 1}{4\pi r_d}\left[\frac{e_{15}^{(1)} p + c_{44}^{(1)} q}{c_{44}^{(1)}\varepsilon_{11}^{(1)} + e_{15}^{(1)} e_{15}^{(1)}}\sin\theta_d - b_\varphi \cos\theta_d\right], \tag{B.4}$$

$$\sigma_{zx}^{T0} = \frac{\lambda - 1}{4\pi r_d}\left[-\sin\theta_d\left(c_{44}^{(1)} b_z + e_{15}^{(1)} b_\varphi\right) - p\cos\theta_d\right], \tag{B.5}$$

$$\sigma_{zy}^{T0} = \frac{\lambda - 1}{4\pi r_d}\left[\cos\theta_d\left(c_{44}^{(1)} b_z + e_{15}^{(1)} b_\varphi\right) - p\sin\theta_d\right], \tag{B.6}$$

$$D_x^{T0} = \frac{\lambda - 1}{4\pi r_d}\left[-\sin\theta_d\left(e_{15}^{(1)} b_z - \varepsilon_{11}^{(1)} b_\varphi\right) + q\cos\theta_d\right], \tag{B.7}$$

$$D_y^{T0} = \frac{\lambda - 1}{4\pi r_d}\left[\cos\theta_d\left(e_{15}^{(1)} b_z - \varepsilon_{11}^{(1)} b_\varphi\right) + q\sin\theta_d\right], \tag{B.8}$$

$$\gamma_{zx}^{Ta} = \frac{\lambda}{4\pi r_d \cos\lambda\theta_d}\left[\frac{e_{15}^{(1)} q - \varepsilon_{11}^{(1)} p}{c_{44}^{(1)}\varepsilon_{11}^{(1)} + e_{15}^{(1)} e_{15}^{(1)}}\sin(\lambda-1)\theta_d + b_z\cos(\lambda-1)\theta_d\right], \tag{B.9}$$

$$\gamma_{zy}^{Ta} = \frac{\lambda}{4\pi r_d \cos\lambda\theta_d}\left[\frac{e_{15}^{(1)} q - \varepsilon_{11}^{(1)} p}{c_{44}^{(1)}\varepsilon_{11}^{(1)} + e_{15}^{(1)} e_{15}^{(1)}}\cos(\lambda-1)\theta_d - b_z\sin(\lambda-1)\theta_d\right], \tag{B.10}$$

$$E_x^{Ta} = \frac{\lambda}{4\pi r_d \cos\lambda\theta_d}\left[\frac{e_{15}^{(1)} p + c_{44}^{(1)} q}{c_{44}^{(1)}\varepsilon_{11}^{(1)} + e_{15}^{(1)} e_{15}^{(1)}}\sin(\lambda-1)\theta_d - b_\varphi\cos(\lambda-1)\theta_d\right], \tag{B.11}$$

$$E_y^{Ta} = \frac{\lambda}{4\pi r_d \cos\lambda\theta_d}\left[\frac{e_{15}^{(1)} p + c_{44}^{(1)} q}{c_{44}^{(1)}\varepsilon_{11}^{(1)} + e_{15}^{(1)} e_{15}^{(1)}}\cos(\lambda-1)\theta_d + b_\varphi\sin(\lambda-1)\theta_d\right], \tag{B.12}$$

$$\sigma_{zx}^{Ta} = \frac{\lambda}{4\pi r_d \cos\lambda\theta_d}\left[\cos(\lambda-1)\theta_d\left(c_{44}^{(1)} b_z + e_{15}^{(1)} b_\varphi\right) - p\sin(\lambda-1)\theta_d\right], \tag{B.13}$$

$$\sigma_{zy}^{Ta} = \frac{-\lambda}{4\pi r_d \cos\lambda\theta_d}\left[\sin(\lambda-1)\theta_d\left(c_{44}^{(1)} b_z + e_{15}^{(1)} b_\varphi\right) + p\cos(\lambda-1)\theta_d\right], \tag{B.14}$$

$$D_x^{Ta} = \frac{\lambda}{4\pi r_d \cos\lambda\theta_d}\left[\cos(\lambda-1)\theta_d\left(e_{15}^{(1)} b_z - \varepsilon_{11}^{(1)} b_\varphi\right) + q\sin(\lambda-1)\theta_d\right], \tag{B.15}$$

$$D_y^{Ta} = \frac{-\lambda}{4\pi r_d \cos\lambda\theta_d}\left[\sin(\lambda-1)\theta_d\left(e_{15}^{(1)} b_z - \varepsilon_{11}^{(1)} b_\varphi\right) - q\cos(\lambda-1)\theta_d\right]. \tag{B.16}$$

References

Bogy, D.B., Wang, K.C., 1971. Stress singularities at interface corners in bonded dissimilar isotropic elastic materials. International Journal of Solids and Structures 7, 993–1005.

Chen, B.J., Xiao, Z.M., Liew, K.M., 2002. On the interaction between a semi-infinite anti-crack and a screw dislocation in piezoelectric solid. International Journal of Solids and Structures 39, 1505–1533.

Chen, D.H., Nisitani, H., 1993. Singular stress fields near the corner of jointed dissimilar materials. Journal of Applied Mechanics 60, 607–613.

Chung, M.Y., Ting, T.C.T., 1995. Line force, charge, and dislocation in anisotropic piezoelectric composite wedges and spaces. ASME Journal of Applied Mechanics 62, 423–428.

Deeg, W.F., 1980. The analysis of dislocation, crack, and inclusion problems in piezoelectric solids. Ph.D Thesis, Stanford University, Stanford, CA.

Lee, K.Y., Lee, W.G., Pak, Y.E., 2000. Interaction between a semi-infinite crack and a screw dislocation in a piezoelectric material. ASME Journal of Applied Mechanics 67, 165–170.

Liu, J.X., Du, S.Y., Wang, B., 1999. A screw dislocation interacting with a piezoelectric bimaterial interface. Mechanics Research Communications 26, 415–420.

Muskhelishvili, N.I., 1975. Some Basic Problems of the Mathematical Theory of Elasticity. Noordhoff International Publishing, Leyden.

Pak, Y.E., 1990a. Force on a piezoelectric screw dislocation. ASME Journal of Applied Mechanics 57, 647–653.

Pak, Y.E., 1990b. Crack extension force in a piezoelectric material. Journal of Applied Mechanics 57, 647–653.

Pahn, L.O., Earmme, Y.Y., 2000. Analysis of a short interfacial crack from the corner of a rectangular inclusion. International Journal of Fracture 106, 341–356.

Reedy, E.D., 2000. Connection between interface corner and interfacial fracture analysis of an adhesively bonded butt joint. International Journal of Solids and Structures 37, 2429–2442.

Reedy, E.D., Guess, T.R., 1997. Interface corner failure analysis of joint strength: effect of adherend stiffness. International Journal of Fracture 88, 305–314.

Xiao, Z.M., Chen, B.J., Fan, H., 2001. An edge dislocation interacting with a wedge-shaped bi-material interface. International Journal of Solids and Structures 38, 8219–8233.